

Anomalous Subthreshold Behaviors in Negative Capacitance Transistors

Yu-Hung Liao, Daewoong Kwon, Suraj Cheema, Ava J. Tan, Ming-Yen Kao, Li-Chen Wang, Chenming Hu, *Life Fellow, IEEE*, and Sayeef Salahuddin, *Fellow, IEEE*,

Abstract—Recent measurements on ultra-thin body Negative Capacitance Field Effect Transistors have shown subthreshold behaviors that are not expected in a classical MOSFET. Specifically, subthreshold swing was found to decrease with increased gate bias in the subthreshold region for devices measured over multiple gate lengths down to 30 nm. In addition, improvement in the subthreshold swing relative to control devices showed a non-monotonic dependence on the gate length. In this paper, using a Landau-Khalatnikov ferroelectric gate stack model calibrated with measured Capacitance-Voltage, we show that both these anomalous behaviors can be quantitatively reproduced with TCAD simulations.

Index Terms—Negative Capacitance, Ferroelectric, Short Channel Effects

I. INTRODUCTION

NEGATIVE capacitance field effect transistors (NCFET) rely on a ferroelectric gate insulator to provide an amplification of the gate signal [1]–[3]. This boost, which depends on the capacitance matching between the ferroelectric and Si underneath, in turn, reduces the power supply voltage requirements. In a properly designed MOSFET, such a boost can also lead to a sub-thermal subthreshold swing (SS). However, the strong function of Si capacitance with voltage and inadequacy of available ferroelectric materials makes it difficult to obtain a sub-thermal subthreshold swing without hysteresis [4], [5]. On the other hand, the objective of reducing supply voltage can be achieved by improving the swing near the threshold and this can be done without violating the condition necessary for zero hysteresis [6]. NCFET so designed can show obvious non-classical behaviors.

Indeed, substantially improved I-V characteristics and non-classical subthreshold behavior have recently been observed in Zr doped HfO₂ gate stack (HZO) [7]–[11] that has a polar order [12], [13]. Despite the same thermal processing, doping, and MOSFET geometry (Fig. 1(a)), the HfO₂ (Control) and HZO (NCFET) gate stack devices demonstrate opposite trends of subthreshold swing with respect to gate bias (Fig. 1(b)) [7]. Figure 2 shows that for all gate lengths (L_G) at $V_{DS}=0.05V$,

Y.-H. Liao, D. Kwon, A. J. Tan, M.-Y. Kao, C. Hu and, S. Salahuddin are with the Department of Electrical Engineering and Computer Sciences, University of California, Berkeley, Berkeley, CA 94720, USA. (e-mail: yh_liao@berkeley.edu).

S. Cheema and L.-C. Wang are with the Department of Material Science and Engineering, University of California, Berkeley, CA 94720, USA.

D. Kwon is now with the Department of Electrical Engineering, Inha University Yonghyeon Campus, Incheon 22212, South Korea

Y.-H. Liao and D. Kwon contributed equally to this work.

This work was supported by the Berkeley Center for Negative Capacitance Transistors.

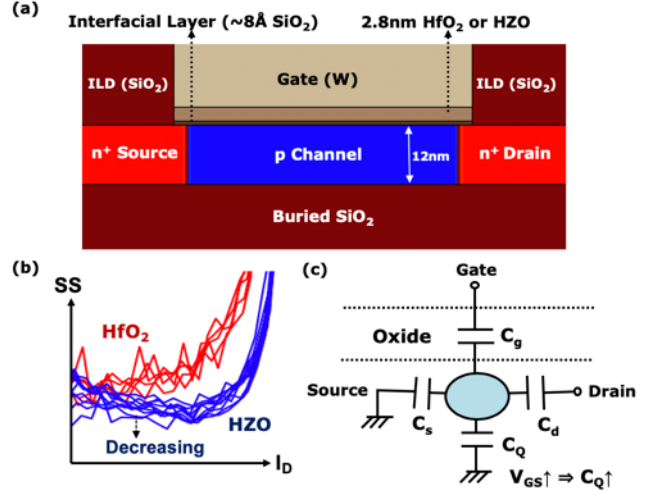


Fig. 1. (a) Schematic cross-section of the SOI n-MOSFETs. Both HfO₂ (Control) and HZO (NC) devices have the same geometry. (b) SS of HfO₂ and HZO devices demonstrating conventional and anomalous trend with respect to I_D , respectively. (c) Equivalent circuit diagram for understanding the MOSFET channel barrier height in subthreshold regime.

the NCFET SS is similar to SS of the Control of the same geometry at low drain current ($I_D=10pA/\mu m$) but is lowered as the gate bias increases. The I_D at which NCFET subthreshold swing reaches its minimum is almost 4 orders of magnitude larger than the OFF current. In addition, the difference in the subthreshold swing between Control and NCFET devices (measured in the range $I_D=0.1nA\sim 1nA/\mu m$) increases significantly from $L_G=100nm$ to $L_G=50nm$ but decreases from $L_G=50nm$ to $L_G=30nm$ (Fig. 3). Remarkably, these two trends for the HZO devices cannot be explained by assuming a “higher- κ ” linear dielectric gate stack which would lead to monotonically increasing improvement of SS as L_G shrinks. Neither are they explainable with a better interface quality than the Control, as it would result in a constant SS reduction over different L_G . In contrast with normal dielectric theory, these anomalies indicate that NCFET gate capacitance (C_g) (Fig. 1(c)) is affected significantly by both V_{GS} and L_G , of which the explanation lies in the non-linear polarization response to the applied electric field for the HZO gate stack layer [4], [14].

II. TCAD MODEL CALIBRATIONS

Sentaurus TCAD [15] simulator parameters are calibrated to C-V and I-V data from [7]. For both Control and NCFET,

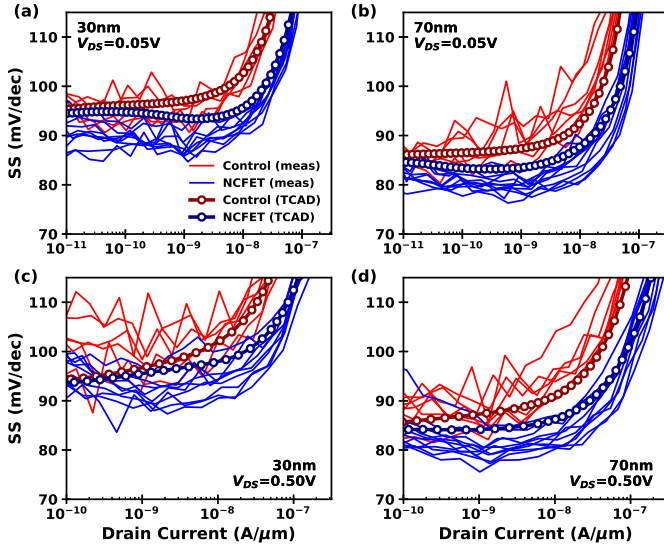


Fig. 2. (a)-(d) Measured and TCAD-simulated SS- I_D relations for Control and NC n-MOSFETs of two gate lengths. Two different drain biases are considered. Multiple devices are measured for each gate length, all of which exhibit negligible hysteresis.

the gate insulator constitutes of a chemical oxide (8) and 2.8nm layer of HfO_2 or HZO. HfO_2 MOSCAP Accumulation C-V measurements can be well matched by a 1.1 nm EOT gate stack in the TCAD model (Fig. 4(a)). The HZO stack demonstrates a higher capacitance which could be fitted with very high dielectric constant for the HZO stack. However, this would require an effective dielectric constant (>100) that is much higher than any theoretical predictions for Hf and Zr-based dielectric phases [16]–[20]. In addition, this hypothetical “super-high κ ” dielectric would not be able to replicate the anomalous subthreshold behaviors that we observed. Instead, the capacitance boost is captured by the potential amplification effect [11], [14], [21] induced by a the presence polar phase inside the HZO layer.

The calibrated simulation reproduces the experimentally observed subthreshold behavior for the Control MOSFET (Fig. 2, 3(a)). NCFETs are simulated by introducing the Landau-Khalatnikov (LK) model for simulating the gate stack, but non-gate-stack parameters are unchanged from the Control devices. The LK parameters are chosen such that the Ferroelectric in the positive capacitance (PC) region results in the same gate stack EOT (1.1 nm) as the Control. Therefore, the SS in the low I_D (10-100pA/ μm) region are matched between Control and NCFET devices. As the gate bias is increased, the Ferroelectric enters into the negative capacitance (NC) region, which results in a reduced gate stack EOT of 0.9nm in accordance with the HZO C-V. This transition from positive to negative capacitance regime successfully captures the near-threshold SS reduction (Fig. 2) with respect to I_D as well as the non-monotonic SS improvement trend with respect to L_G (Fig. 3(b) inset). This is discussed in more details later.

III. RESULTS AND DISCUSSIONS

Fig. 4(b) shows threshold voltage (V_t) calibration results with tungsten work-function set to 4.6eV according to C-

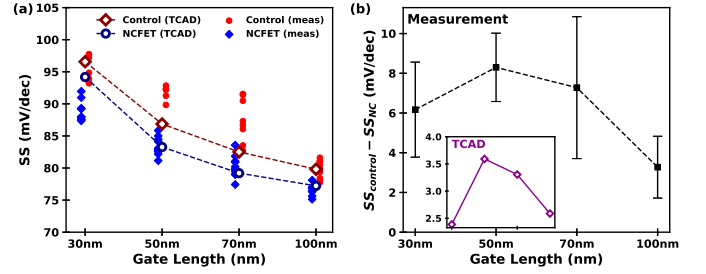


Fig. 3. (a) SS averaged over $I_D=0.1\sim 1\text{nA}/\mu\text{m}$ at $V_{DS}=0.05\text{V}$ for measured and TCAD-simulated Control and NC MOSFET. Each marker presents one device having the corresponding gate length. (b) Experimentally estimated SS improvement for different gate lengths. Each error bar presents the estimated mean and one standard deviation. (Inset) TCAD-modeled Improvements for the four gate lengths.

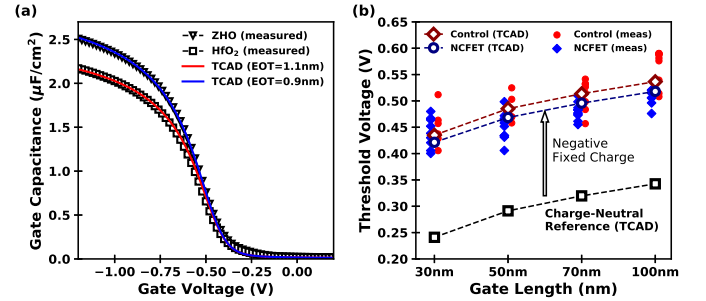


Fig. 4. (a) Measured and TCAD-simulated C-V for p-type doped MOS capacitors with HfO_2 and ZHO gate stacks. (b) Constant-current ($I_D=10\text{nA}/\mu\text{m}$) threshold voltage (V_t) at $V_{DS}=0.05\text{V}$ for measured and TCAD-simulated Control and NC MOSFET. Each marker represents an extraction for one device. Experimental V_t are 0.18V larger than simulated V_t without interface charge. The discrepancy is resolved when $-0.6\mu\text{C}/\text{cm}^2$ fixed charge is added to the Si/SiO₂ interface.

V calibrations (Fig. 4(a)). Note that Control MOSFET V_t would be underestimated by 0.18V if no net defect charges are assumed, and this discrepancy is insensitive to geometry and doping profiles when SS scaling trend is captured. Therefore, the difference between the MOSCAP and MOSFET V_{FB} is ascribed to additional defect charges introduced by transistor fabrication processes. A fixed charge density of $-0.6\mu\text{C}/\text{cm}^2$ at the Si/SiO₂ interface can not only account for the V_t shift but also explain the small measured V_t difference between Control and NC devices (Fig. 4(b)). The voltage drop on the gate stack induced by the charges is less for the NCFET than the Control because of its larger C_g , which results in a lower V_t that is consistent with the experiments. On the other hand, if there were no fixed charges, the NCFET V_t would be larger than the Control V_t because of mitigated short channel effects. Note that, the introduction of negative fixed charges into the model is consistent with our previous work as described in [22] where the transistor fabrication followed essentially the exact same procedure.

Fig. 5 shows the transitions from positive to negative capacitance region of the HZO stack. When V_{GS} ramps up, both I_D and the external electric field on the gate stack ($E_{ext} = Q_G/\epsilon_0$) increases. The HZO polarization is directly determined by E_{ext} if polarization gradient energy is negligible. The Q_G - I_D slope in the subthreshold regime is associated

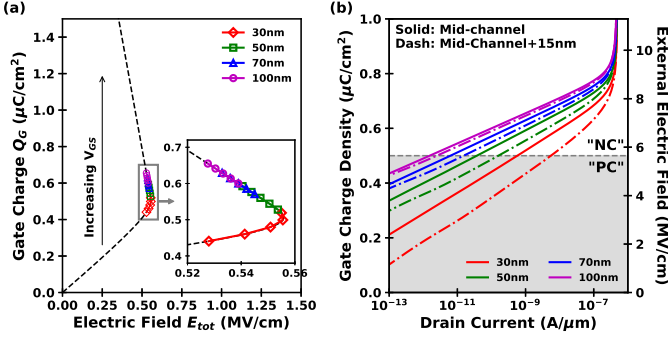


Fig. 5. (a) Extracted Q-E relation for the polar layer of the gate stack at the mid-channel of NCFETs at $V_{DS}=50\text{mV}$. For each gate length, the gate voltage is ramped at which I_D is from $0.1\text{nA}/\mu\text{m}$ to $1\text{nA}/\mu\text{m}$. (b) Simulated relations between drain current and (left axis) local gate charge density / (right axis) local external electric field at $V_{DS}=0.05\text{V}$ for NCFETs. For each gate length, the solid line is extracted at mid-channel gate stack region, and the dash line is extracted at the region 15nm laterally from mid-channel toward the drain. The white-background region corresponds to bias conditions at which the polar layer exhibits negative capacitance, while the dark background stands for positive-capacitance regime.

with input capacitance $C_{gg} = \left(\frac{1}{C_g} + \frac{1}{C_s + C_d + C_Q}\right)^{-1}$, which increases for reduced L_G because of C_s and C_d increase. As the device enters the negative capacitance region, a voltage amplification ensues and drives down the subthreshold swing. This explains why, for the NCFET, the subthreshold swing gets steeper in the sub-threshold regime as V_{GS} or I_D increases. To fully understand the observed anomalous behaviors, especially the effect of L_G , one needs to consider the inner fringing field that plays a crucial role on the capacitance matching effect [22], [23]. This field leads to the gate stack-to-source and gate stack-to-drain capacitive coupling which reduces Q_G to balance the positively ionized source and drain donor charges for n-MOSFET in subthreshold regime. When L_G shrinks, mid-channel Q_G corresponding to the same I_D decreases because of the increased inner fringing field. As a result, although the mid-channel gate stack is in the negative capacitance regime for L_G from 50nm to 100nm at $I_D=0.1\text{nA}/\mu\text{m}$, it remains in the positive capacitance regime for the 30nm case (Fig. 5). Therefore, the improvement in the subthreshold swing for NCFETs drops for $L_G=30\text{nm}$ as shown in Fig. 3(b).

Notably, the extracted Q_G at which the HZO gate stack starts to exhibit negative capacitance is approximately $0.5\mu\text{C}/\text{cm}^2$ (Fig. 5(a)). In other words, the S curve is pushed up in the charge axis. This is a consequence of the negative fixed charge that simultaneously explains the V_t trend for both Control and the NCFET. The atypical response can be a result of antiferroelectric behavior of the tetragonal phase [13] in the HZO or a small but finite leakage that induces positive charge trapping at the SiO_2/HZO interface and effectively shifts the S-curve [24], [25].

IV. CONCLUSION

To summarize, we developed an FE model that simultaneously explains (i) SS getting steeper with increasing I_D in the subthreshold regime, and (ii) non-monotonic behavior of SS improvement with L_G trends that cannot be explained by a classical “high- κ ” scaling theory. Our results show that

the capacitance matching leads to (i), while the inner fringe field induces change in the capacitance matching in short channel MOSFETs and leads to (ii). This model supports the notion that Ferroelectric material optimization with appropriate device design [26] to maximize near threshold capacitance matching may lead to significant reduction in V_{DD} .

REFERENCES

- [1] S. Salahuddin and S. Datta, "Use of negative capacitance to provide voltage amplification for low power nanoscale devices," *Nano Lett.*, vol. 8, no. 2, pp. 405–410, 2008.
- [2] S. Salahuddin and S. Datta, "Can the subthreshold swing in a classical fet be lowered below 60 mv/decade?" in *2008 IEEE International Electron Devices Meeting*, 2008, pp. 1–4.
- [3] Z. Krivokapic, U. Rana, R. Galatage, A. Razavieh, A. Aziz, J. Liu, J. Shi, H. J. Kim, R. Sporer, C. Serrao, A. Busquet, P. Polakowski, J. Miller, W. Kleemeier, A. Jacob, D. Brown, A. Knorr, R. Carter, and S. Banna, "14nm ferroelectric finfet technology with steep subthreshold slope for ultra low power applications," in *2017 IEEE International Electron Devices Meeting (IEDM)*, 2017, pp. 15.1.1–15.1.4.
- [4] J. C. Wong and S. Salahuddin, "Negative capacitance transistors," *Proceedings of the IEEE*, vol. 107, no. 1, pp. 49–62, Jan 2019.
- [5] H. Agarwal, P. Kushwaha, Y.-K. Lin, M.-Y. Kao, Y.-H. Liao, A. Dasgupta, S. Salahuddin, and C. Hu, "Proposal for capacitance matching in negative capacitance field-effect transistors," *IEEE Electron Device Letters*, vol. 40, no. 3, pp. 463–466, 2019.
- [6] A. I. Khan, C. W. Yeung, C. Hu, and S. Salahuddin, "Ferroelectric negative capacitance MOSFET: Capacitance tuning & antiferroelectric operation," in *Electron Devices Meeting (IEDM), 2011 IEEE International*, 2011, pp. 11–3.
- [7] D. Kwon, S. Cheema, Y. Lin, Y. Liao, K. Chatterjee, A. J. Tan, C. Hu, and S. Salahuddin, "Near threshold capacitance matching in a negative capacitance fet with 1 nm effective oxide thickness gate stack," *IEEE Electron Device Letters*, vol. 41, no. 1, pp. 179–182, 2020.
- [8] D. Kwon, S. Cheema, N. Shanker, K. Chatterjee, Y. Liao, A. J. Tan, C. Hu, and S. Salahuddin, "Negative capacitance fet with 1.8-nm-thick zr-doped hfo2 oxide," *IEEE Electron Device Letters*, vol. 40, no. 6, pp. 993–996, 2019.
- [9] W. Chung, M. Si, and P. D. Ye, "Hysteresis-free negative capacitance germanium cmos finfets with bi-directional sub-60 mv/dec," in *2017 IEEE International Electron Devices Meeting (IEDM)*, 2017, pp. 15.3.1–15.3.4.
- [10] Z. Yu, H. Wang, W. Li, S. Xu, X. Song, S. Wang, P. Wang, P. Zhou, Y. Shi, Y. Chai, and X. Wang, "Negative capacitance 2d mos2 transistors with sub-60mv/dec subthreshold swing over 6 orders, 250 a/m current density, and nearly-hysteresis-free," in *2017 IEEE International Electron Devices Meeting (IEDM)*, 2017, pp. 23.6.1–23.6.4.
- [11] J. Zhou, G. Han, Q. Li, Y. Peng, X. Lu, C. Zhang, J. Zhang, Q. Sun, D. W. Zhang, and Y. Hao, "Ferroelectric hfxrox ge and gesn pmosfets with sub-60 mv/decade subthreshold swing, negligible hysteresis, and improved ids," in *2016 IEEE International Electron Devices Meeting (IEDM)*, 2016, pp. 12.2.1–12.2.4.
- [12] X. Sang, E. D. Grimley, T. Schenk, U. Schroeder, and J. M. LeBeau, "On the structural origins of ferroelectricity in hfo2 thin films," *Applied Physics Letters*, vol. 106, no. 16, p. 162905, 2015. [Online]. Available: <https://doi.org/10.1063/1.4919135>
- [13] M. H. Park, Y. H. Lee, H. J. Kim, Y. J. Kim, T. Moon, K. D. Kim, J. Miller, A. Kersch, U. Schroeder, T. Mikolajick, and C. S. Hwang, "Ferroelectricity and antiferroelectricity of doped thin hfo2-based films," *Advanced Materials*, vol. 27, no. 11, pp. 1811–1831, 2015.
- [14] M. Hoffmann, F. P. G. Fegler, M. Herzig, T. Mittmann, B. Max, U. Schroeder, R. Negrea, P. Lucian, S. Slesazek, and T. Mikolajick, "Unveiling the double-well energy landscape in a ferroelectric layer," *Nature*, vol. 565, no. 7740, pp. 464–467, 2019. [Online]. Available: <https://doi.org/10.1038/s41586-018-0854-z>
- [15] *SentaurusTM Device User Guide, Version O-2018.06*. Synopsys, Inc, Jun 2018.
- [16] G.-M. Rignanese, X. Gonze, G. Jun, K. Cho, and A. Pasquarello, "First-principles investigation of high- κ dielectrics: Comparison between the silicates and oxides of hafnium and zirconium," *Phys. Rev. B*, vol. 69, p. 184301, May 2004. [Online]. Available: <https://link.aps.org/doi/10.1103/PhysRevB.69.184301>
- [17] X. Zhao, D. Ceresoli, and D. Vanderbilt, "Structural, electronic, and dielectric properties of amorphous ZrO₂ from ab initio molecular dynamics," *Phys. Rev. B*, vol. 71, p. 085107, Feb 2005. [Online]. Available: <https://link.aps.org/doi/10.1103/PhysRevB.71.085107>
- [18] T.-J. Chen and C.-L. Kuo, "First principles study of the structural, electronic, and dielectric properties of amorphous hfo2," *Journal of Applied Physics*, vol. 110, no. 6, p. 064105, 2011. [Online]. Available: <https://doi.org/10.1063/1.3636362>
- [19] D. Fischer and A. Kersch, "The effect of dopants on the dielectric constant of hfo2 and zro2 from first principles," *Applied Physics Letters*, vol. 92, no. 1, p. 012908, 2008. [Online]. Available: <https://aip.scitation.org/doi/abs/10.1063/1.2828696>
- [20] G. Dutta, K. P. S. S. Hembram, G. M. Rao, and U. V. Waghmare, "Effects of o vacancies and c doping on dielectric properties of zro2: A first-principles study," *Applied Physics Letters*, vol. 89, no. 20, p. 202904, 2006. [Online]. Available: <https://doi.org/10.1063/1.2388146>
- [21] W. Gao, A. Khan, X. Marti, C. Nelson, C. Serrao, J. Ravichandran, R. Ramesh, and S. Salahuddin, "Room-temperature negative capacitance in a ferroelectric/dielectric superlattice heterostructure," *Nano Letters*, vol. 14, no. 10, pp. 5814–5819, 2014, pMID: 25244689. [Online]. Available: <https://doi.org/10.1021/nl502691u>
- [22] Y. Liao, D. Kwon, Y. Lin, A. J. Tan, C. Hu, and S. Salahuddin, "Anomalously beneficial gate-length scaling trend of negative capacitance transistors," *IEEE Electron Device Letters*, vol. 40, no. 11, pp. 1860–1863, 2019.
- [23] Y. Lin, H. Agarwal, P. Kushwaha, M. Kao, Y. Liao, K. Chatterjee, S. Salahuddin, and C. Hu, "Analysis and modeling of inner fringing field effect on negative capacitance finfets," *IEEE Transactions on Electron Devices*, vol. 66, no. 4, pp. 2023–2027, April 2019.
- [24] A. I. Khan, U. Radhakrishna, S. Salahuddin, and D. Antoniadis, "Work function engineering for performance improvement in leaky negative capacitance fets," *IEEE Electron Device Letters*, vol. 38, no. 9, pp. 1335–1338, 2017.
- [25] A. I. Khan, U. Radhakrishna, K. Chatterjee, S. Salahuddin, and D. A. Antoniadis, "Negative capacitance behavior in a leaky ferroelectric," *IEEE Transactions on Electron Devices*, vol. 63, no. 11, pp. 4416–4422, 2016.
- [26] H. Agarwal, P. Kushwaha, J. P. Duarte, Y. Lin, A. B. Sachid, H. Chang, S. Salahuddin, and C. Hu, "Designing 0.5 v 5-nm hp and 0.23 v 5-nm lp nc-finets with improved I_{OFF} sensitivity in presence of parasitic capacitance," *IEEE Transactions on Electron Devices*, vol. 65, no. 3, pp. 1211–1216, 2018.